Protoplasma (1991) 163: 51–61

PROTOPLASMA

Isolation of F-actin from pea stems

Evidence from fluorescence microscopy

Shunnosuke Abe** and **E. Davies***

School of Biological Sciences, University of Nebraska-Lincoln, Lincoln, Nebraska

Received August 24, 1990
Accepted January 14, 1991

Summary. A procedure is introduced which allows the isolation of abundant amounts of F-actin from plants (etiolated pea seedlings) in an array of morphologies very similar to the array of morphologies found in situ. The major feature is a homogenizing medium containing very low ionic strength, low monovalent ion (K^+) concentration, a 3-fold higher level of Mg^{++}, the presence of EGTA to chelate Ca^{++}, and PMSF to inhibit protease activity. Using this buffer, about 80–90% of the sedimentable actin is found in the low speed (4,000 × g) pellet.

Keywords: F-actin isolation; Rhodamine-phalloidin; Fluorescein-S_1-myosin; Fluorescence microscopy.

Abbreviations: CSB cytoskeleton-isolation buffer; DTE dithioerythritol; EGTA ethylene-glycol-bis(B-aminoethyl ether) N,N,N'N'-tetraacetic acid; EPPS N-[2-hydroxyethyl]-piperazine-N'-[3-propane-sulfonic acid]; HEPES N-[hydroxyethyl]-piperazine-N'-[2-ethanesulfonic acid]; MFSB microfilament-stabilizing buffer; PIPES piperazine-N,N'-bis[2-ethanesulfonic acid]; PMSF phenylmethylsulfonyl fluoride; PTE polyoxyethylene-10-tridecyl ether; TRIS tris-(hydroxymethyl) aminoethane.

Introduction

The cytoskeleton in animal tissues consists of microfilaments, composed of actin; actin-binding proteins or microfilament-associated proteins; microtubules, composed of tubulin, and intermediate filaments, composed of numerous different proteins in different tissues (Bershadsky and Vasilev 1988). The cytoskeleton in plants is known to consist of microfilaments and microtubules, but little is known about microfilament-associated proteins or intermediate filaments (Seagull 1989).

* Correspondence and reprints: School of Biological Sciences, University of Nebraska-Lincoln, Lincoln, NE 68588-0118, U.S.A.
** Permanent address: Laboratory of Biochemistry, Department of Biological Resources, College of Agriculture, Ehime University, Tarumi, Matsuyama, Japan.

Much of the information concerning microfilament-associated proteins in animal tissues has come from studies in which actin was isolated in filamentous form (F-actin) and proteins binding to these filaments were identified. We are aware of no such studies with higher plant tissues, presumably because methods do not exist for the isolation of abundant amounts of F-actin.

It is perhaps in studies of this nature that the greatest differences lie in the methodologies employed with plant and animal tissues. Studies on the animal cytoskeleton frequently employ cell cultures for which it is necessary merely to use gentle detergent extraction to isolate apparently intact cytoskeletons (Lenk et al. 1977); in contrast, multicellular animal tissues are thought to be much more difficult for cytoskeleton isolation (Capco et al. 1987). In higher plants, the situation is far more complex, since not only are the tissues multicellular, but each cell is surrounded by its own, individual, tough cell wall, and this cell wall must be ruptured in order to release sub-cellular components. Unfortunately, methods which permit disruption of the cell wall also disrupt the vacuolar membrane, thereby releasing potentially-noxious compounds into the cell extract. It is because of the massive volume and contents of the vacuole that a truly "physiological" buffer (as employed by animal workers) is impossible to attain with higher plants. Efforts to circumvent disruption of the cell wall (and hence of the vacuole) by using protoplasts may also furnish misleading results, since the act of converting cells to protoplasts causes changes in the appearance of the cytoskeleton.

Microfilaments (filamentous actin, or F-actin) have frequently been identified in situ in plant tissues, originally

using electron microscopy of negatively-stained or heavy meromyosin-labelled samples (Staiger and Schliwa 1987) and more recently with fluorescence microscopy employing, for instance, rhodamine-phalloidin (Nothnagel et al. 1981, Parthasarathy 1985). Monomeric actin (globular or G-actin) has been isolated from plant tissues on numerous occasions, generally using rather low ionic strength buffers (Vahey and Scordilis 1980, Ma and Yen 1989).

To our knowledge, however, F-actin in the form of microfilaments has not been isolated from higher plant tissues in abundant amounts, yet such isolation methods would appear to be a prerequisite for identifying actin-binding proteins and any other cellular components that might associate in vivo with microfilaments. Accordingly, the studies reported here were conducted with the intent of finding a homogenization medium that would allow the isolation of (fragments of) F-actin from a particular plant tissue (pea epicotyl) with a view to future studies on the identification of components associated with these F-actin microfilaments.

Materials and methods

The third internode of etiolated pea plants (*Pisum sativum* var. Alaska) grown as described earlier (Davies and Schuster 1981) was used throughout. Hand sections at least 2–3 cells thick were cut and fixed immediately for 10 min in one of a variety of solutions: 2% paraformaldehyde in the high ionic strength microfilament stabilizing buffer (MFSB) of Traas et al. (1987), which contains 100 mM PIPES, adjusted to pH 7.0 with 165 mM NaOH, 5 mM $MgSO_4$, 10 mM EGTA, and modified here by the addition of 1.0 mM PMSF and 0.5% of the non-ionic detergent, PTE; 2% paraformaldehyde in our low ionic strength cytoskeleton-isolation buffer (CSB) consisting of 5 mM HEPES, 3.2 mM KOH, 10 mM Mg acetate, 2 mM EGTA, 1 mM PMSF, 0.5% PTE, pH 7.5; or directly in CSB, i.e., without paraformaldehyde. The fixed sections were then rinsed twice in CSB containing 20 mM DTE and stained for 15 min in 330 nM rhodamine-phalloidin (Molecular Probes Inc, R415) in the same buffer without detergent. Aliquots of the stain were dried in vacuo and the dye reconstituted in the appropriate aqueous medium following the manufacturers' suggested procedure (Molecular Probes Inc).

After staining, the sections were placed individually on microscope slides in a solution containing 50 mM EPPS (pH 8.2), 2 mM EGTA, 10 mM MG acetate, 50 mM DTE and 90% glycerol (Picciolo and Kaplan 1984) and cover slips sealed with nail polish. We substituted EPPS, a zwitterionic biological buffer, in place of Tris, as recommended in the original method, because we found Tris caused disruption of the cytoskeleton in peas. The sections were deliberately made more than one cell thick so that the cytoplasmic contents would not be lost, even though this prevented clear visualization of filaments in individual cells. Fluorescence of rhodamine-phalloidin was observed with an epifluorescence microscope (Nikon) equipped with a 546 nm excitation filter and a 580 nm barrier filter.

Visualization of microfilaments in pea homogenates and various subfractions also generally employed rhodamine-phalloidin. Stock solutions of the strain (generally 5 µl) were dried in vacuo in a microfuge tube and 10 µl of the various sub-fractions directly added to the tube and placed on ice. After 10–20 min incubation on ice, a small aliquot of DTE was added to a final concentration of 200 mM as an anti-fading agent (Picciolo and Kaplan 1984). We found that this high concentration of DTE gave slightly lower initial fluorescence than did 20 mM, but was much more efficient at preventing fading, so that slides could be scanned slowly to locate regions showing typical patterns of fluorescence. This high concentration of DTE did not seem to affect the appearance of microfilaments. A drop of about 4 µl of the stained sample was placed on a slide, covered immediately with a cover slip and sealed with nail polish. When prepared in this way we could obtain more than 20-fold brighter fluorescence than with conventional staining methods and the slides were stable for at least a week. In contrast, we found that conventional, glycerol-based sealing solutions containing n-propyl gallate as an anti-fading agent (Giloh and Sedat 1982) gave poor staining, high background and artefactual aggregation of microfilament-containing structures.

Specificity of labelling was tested both by using unlabelled phalloidin as a blocking agent to assure that the material did, indeed, consist of microfilaments (Schmit and Lambert 1987) and by the use of an alternative probe, fluorescein-S_1-myosin in accordance with manufacturers' directions (Wako Industries, Hiroshima, Japan). Fluorescence of fluorescein-myosin was observed under a blue (490 nm) excitation filter and a barrier-pass filter of 520–560 nm.

Photographs were taken using an automatic camera system (Nikon, UFX II) using black and white film (Kodak Tri-X Pan 400). Exposure time was generally less than 1 sec at maximum excitation.

For protein extraction and gel electrophoresis, samples were ground in 10 volumes of CSB containing 0.5% PTE, filtered through Miracloth and centrifuged at 120 × **g** for 5 min to pellet debris. The supernatant was then centrifuged at 4,000 × **g** for 15 min, and the resulting supernatant was centrifuged at 15,000 × **g** for 15 min. The pellets were resuspended in 0.1 vols. CSB + PTE and then equal volumes of 2 × sample buffer (4% lithium dodecyl sulphate, 4% 2-mercaptoethanol, 40 mM Tris-HCl, pH 6.8) added to the resuspended pellets and supernatant fractions. Immediately prior to electrophoresis, samples were heated at 100 °C for 3 min. Proteins were

Fig. 1. Microfilaments in pea epicotyl tissue visualized in situ. Longitudinal free-hand sections were prepared from dark-grown pea epicotyls, fixed with 2% paraformaldehyde in conventional microfilament-stabilizing buffer (Traas et al. 1987), stained with rhodamine-phalloidin, immersed in glycerol in the presence of n-propyl gallate as an anti-fading reagent and then sealed under a cover slip with nail polish prior to viewing under epifluorescence. **A** From vascular region; **B** as in **A**, but higher magnification of actin cables in vascular cells; **C** tissue as in A, but fixed in paraformaldehyde in CSB; or **D** examined directly after permeabilizing in CSB in the absence of paraformaldehyde; **E** parenchyma tissue, but stained in CSB without fixation (as in **D**). Bars: A and C–E, 40 µm; B, 16 µm. **B** The white arrow indicates actin cables; the black arrow actin bundles; arrowheads sharp, bent filaments; curved arrow looped filaments; open arrow irregularly-angled filament. **E** White arrow indicates filaments coalesced around one nucleus; black arrow crenulated filament; open arrow web-like filaments over another nucleus (*n*)

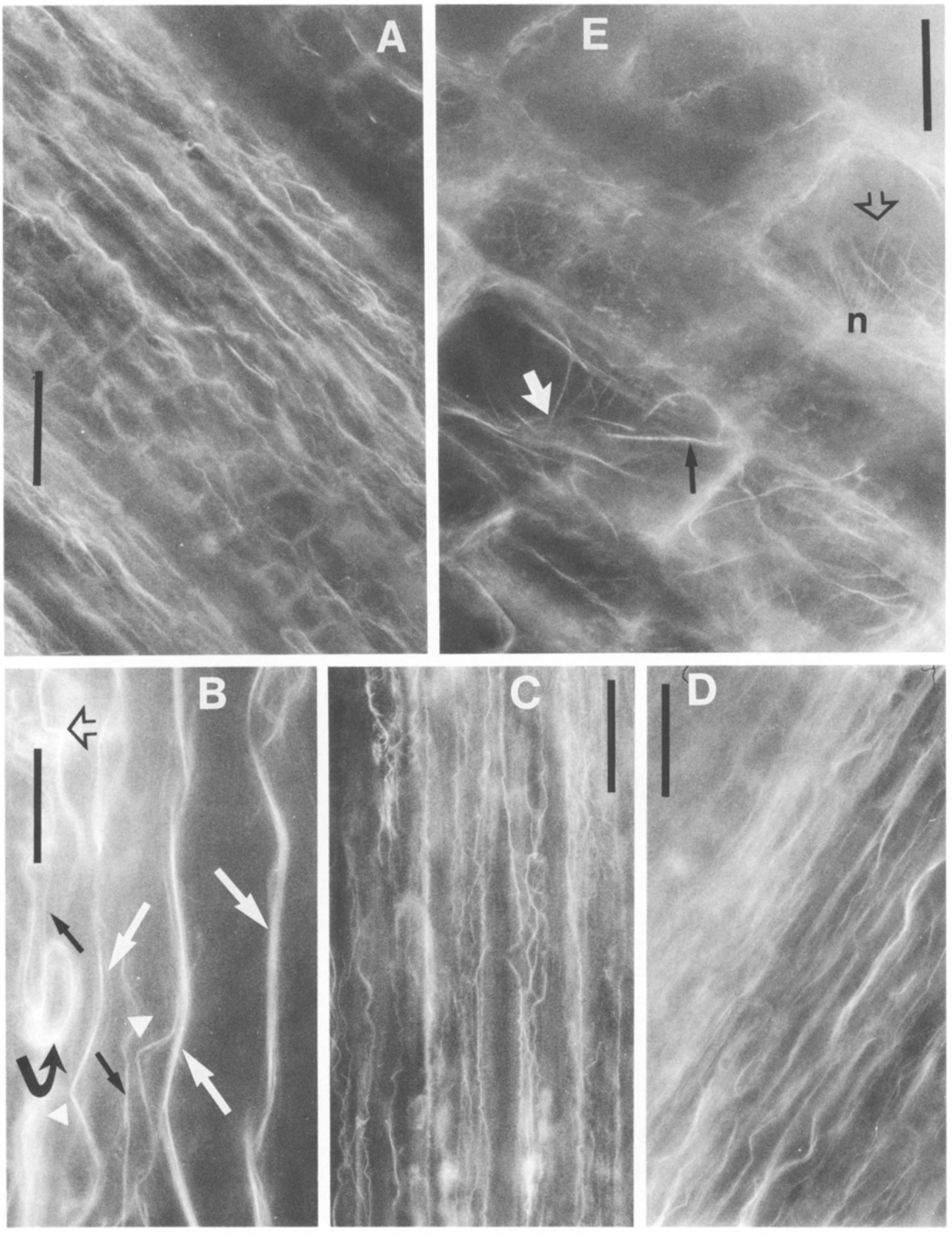
A
E
n
B
C
D

electrophoretically separated in a 10% polyacrylamide gel as described earlier (Schuster and Davies 1983) and stained with Coommassie Brilliant Blue R-250.

For Western blots, proteins separated on gels were electrophoretically transferred to PVDF membranes (Millipore Corp) in electrophoresis buffer containing 10% methanol using a semi-dry blotter for 35 min at 2 mA/cm^2. Detection of actin protein was done using a streptavidin-biotin conjugated system obtained from Amersham with a mouse monoclonal antibody against chicken gizzard actin as a primary antibody. The standard actin protein from chicken gizzard was obtained from Sigma and treated in the same manner as pea extracts for electrophoresis.

Results

Microfilament morphology in tissue sections

Conventional methods for identifying microfilaments in plant tissues involve fixation of tissue slices in paraformaldehyde prior to staining with rhodamine-phalloidin in a high ionic strength buffer such as MFSB (Traas et al. 1987). Using such methods with slight modifications as described in the Materials and methods, it can be seen (Fig. 1 A and B) that pea epicotyls contain filaments very similar to those in monocotyledons (Parthasarathy 1985). In vascular cells, many filaments appear to extend the entire length of the cell when compared with a bright field view (picture not shown) and often to be in excess of 100 μm in length (Fig. 1 A) and, as judged from fluorescent images at higher magnification, between 200 nm (actin bundles?; Fig. 1 B, arrow) and 700 nm (actin cables?; Fig. 1 B, arrowhead) in diameter. These filaments were of at least two types; thicker ones, either closely underlying the plasma membrane and especially evident in vascular cells (Fig. 1 B); and thinner ones traversing the cytoplasmic interior (Fig. 1 A). Some of these filaments appear to be more-or-less straight, others are angular, yet others are formed into circles or spirals (Fig. 1 B especially).

Similar tissue fixed in CSB in the presence of paraformaldehyde (Fig. 1 C) yielded fluorescence patterns very similar to those in MFSB (Fig. 1 A and B), except that more, finer structures were visible with CSB. Using unfixed cells, detergent-permeabilized in CSB, delicate microfilaments were frequently seen traversing the cell interior (Fig. 1 D and E), often appearing to enclose the nucleus in parenchyma cells (Fig. 1 E, white arrow). In these unfixed cells, some filaments appeared crenulated (Fig. 1 E, black arrow) similar to those described by Parthasarathy (1985) and others show a criss-crossing network with the appearance of dots at cross-over points (Fig. 1 E, open arrow).

It is apparent from these pictures that pea epicotyls contain various types of microfilaments which can be visualized in fixed or unfixed tissue using conventional buffers (MSFB) or the low ionic strength CSB developed here. These filaments vary in length, thickness and shape with the most varied array, especially of very fine filaments, being seen in parenchyma cells stained in CSB without fixative (Fig. 1 E). These patterns are quite similar to those seen in unfixed cells of *Chara* and *Funaria* (Tewinkel et al. 1989).

Microfilament morphology in extracts

Figure 2 shows typical views of resuspended pellets from tissue homogenized in either the conventional high ionic strength microfilament-stabilizing buffer (Traas et al. 1987) supplemented with 0.5% PTE to solubilize membranes and 1 mM PMSF to inhibit endogenous proteases (Fig. 2 A) or in the low ionic strength CSB developed here (Fig. 2 B). Short fragments of rather thick filaments (presumably bundles) were seen, but thin filaments, as seen in situ (Fig. 1), were rare in tissue ground in the high ionic strength buffer (Fig. 2 A). In contrast, numerous filaments were present, densely distributed throughout the entire area of the resuspended pellet from tissue ground in low ionic strength CSB (Fig. 2 B). This pellet constitutes, therefore, a fraction highly enriched in (fragmented) microfilaments. These filaments were not always resolved because they frequently overlapped and their diameters (200–300 nm) were often close to the resolution of the light microscope; others, however, were as much as 700 nm in diameter and appeared to resemble the actin cables visualized in situ (Fig. 1). Some filaments were about 40 μm long (Fig. 2 B, arrow), while others were less than 1 μm and presumably resulted from fragmentation occurring during tissue homogenization. Some of these filaments appeared similarly crenulated (Fig. 2 B, arrow) to those seen in situ (Fig. 1 E), while others were curved, angled, or linear.

Fig. 2. Microfilaments in homogenates and in low speed pellets. Similar tissue to that used in Fig. 1 was ground in 10 volumes of either: **A** the high ionic strength buffer of Traas et al. (1987); or **B–H** low ionic strength buffer (CSB). The homogenate was filtered through miracloth and either: **C–H** examined directly after being filtered; or **A** and **B** after centrifuging the filtrate at 4,000 × **g** for 25 min to obtain low speed pellets. The pellets were gently resuspended in their original buffers prior to staining while the homogenates were stained directly with rhodamine-phalloidin with 0.2 M DTE as an anti-fading agent. Bars: A and B, 20 μm; C–H, 10 μm. **B** Long, white arrow indicates filament at least 40 μm long; curved arrow crenulated filament. **C** Small, bright spots on a crenulated filament

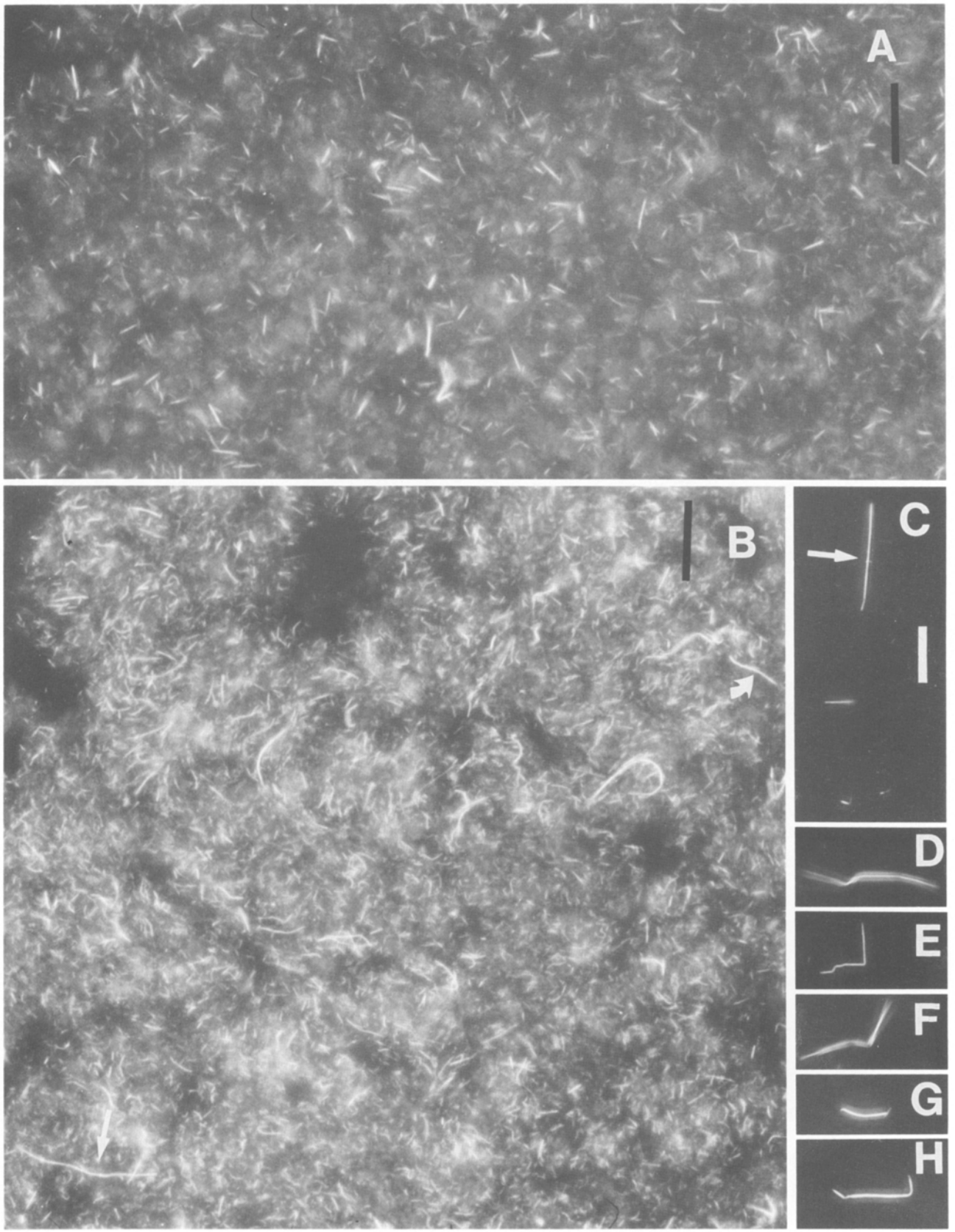
A
B
C
D
E
F
G
H

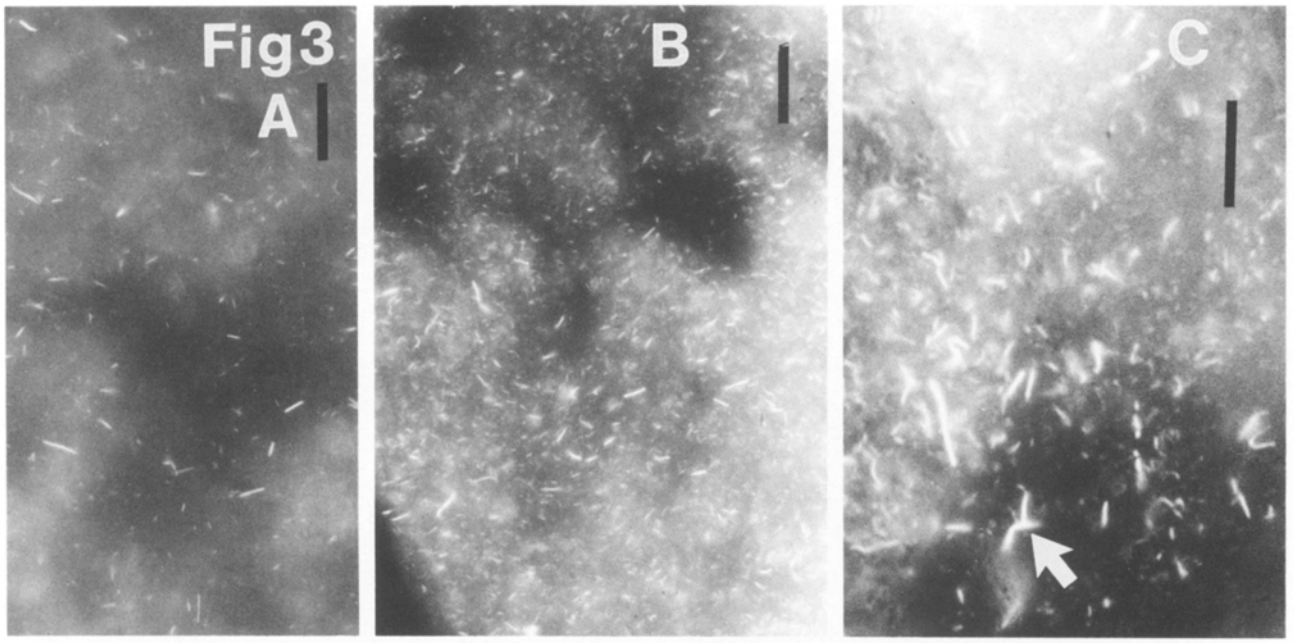

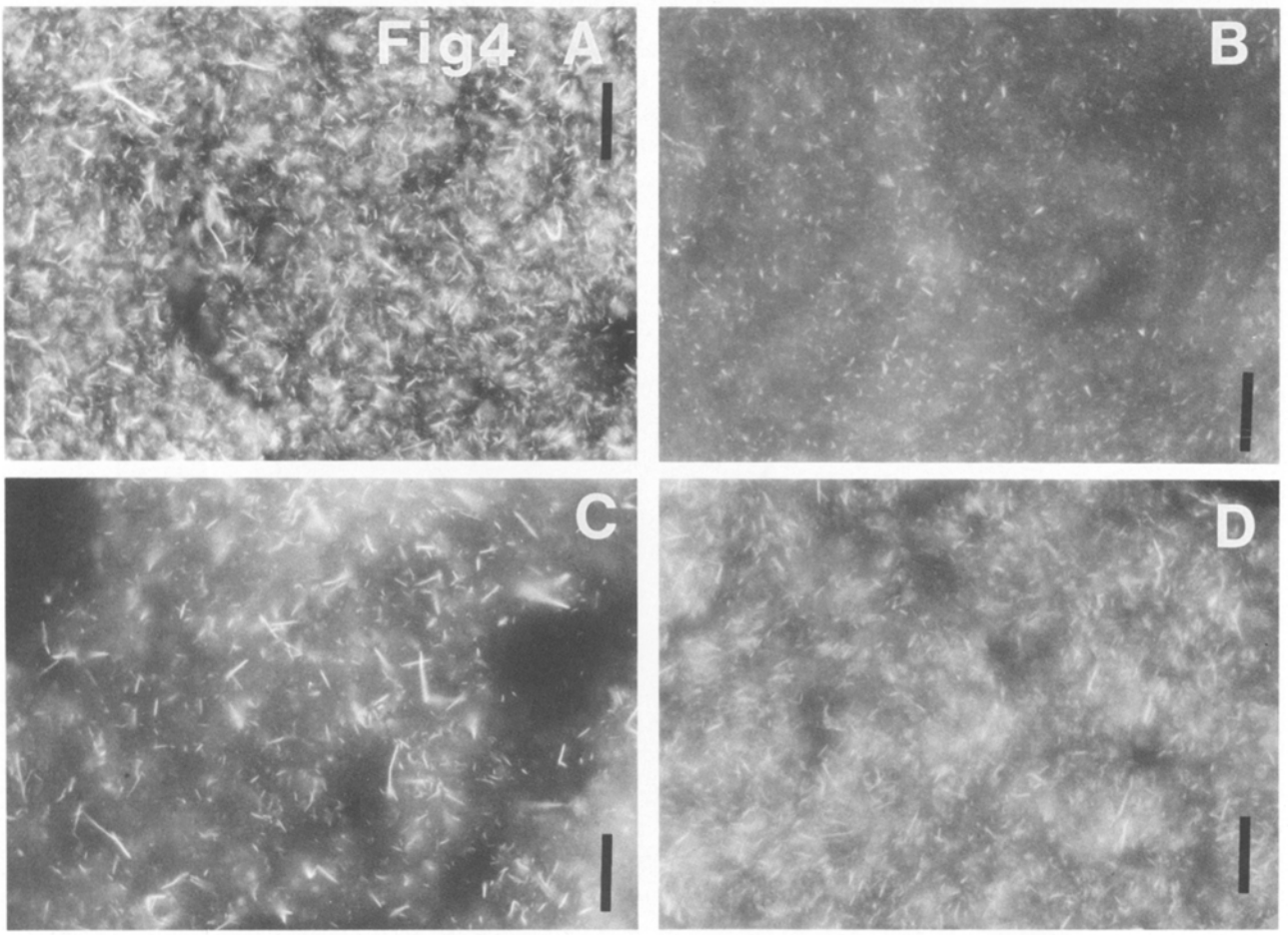

Fig. 3. Effect of Mg^{++} concentration on the yield and appearance of isolated microfilaments. Tissue was ground in CSB except that the concentration of Mg^{++} was: **A** 3 mM; or **B** and **C** 50 mM, and processed as in Fig. 2B. Bars: 10 μm. **C** White arrow points to aggregated cable-like structures

Fig. 4. Effect of Mg^{++} and centrifugal force on the yield and appearance of isolated microfilaments. Tissue was homogenized and processed as in Fig. 3, except that the Mg^{++} concentration and centrifugal forces were varied as follows: **A** 10 mM, 4,000 × **g**; **B** 10 mM, 15,000 × **g**; **C** 5 mM, 4,000 × **g**; **D** 5 mM, 15,000 × **g**. Bars: 10 μm

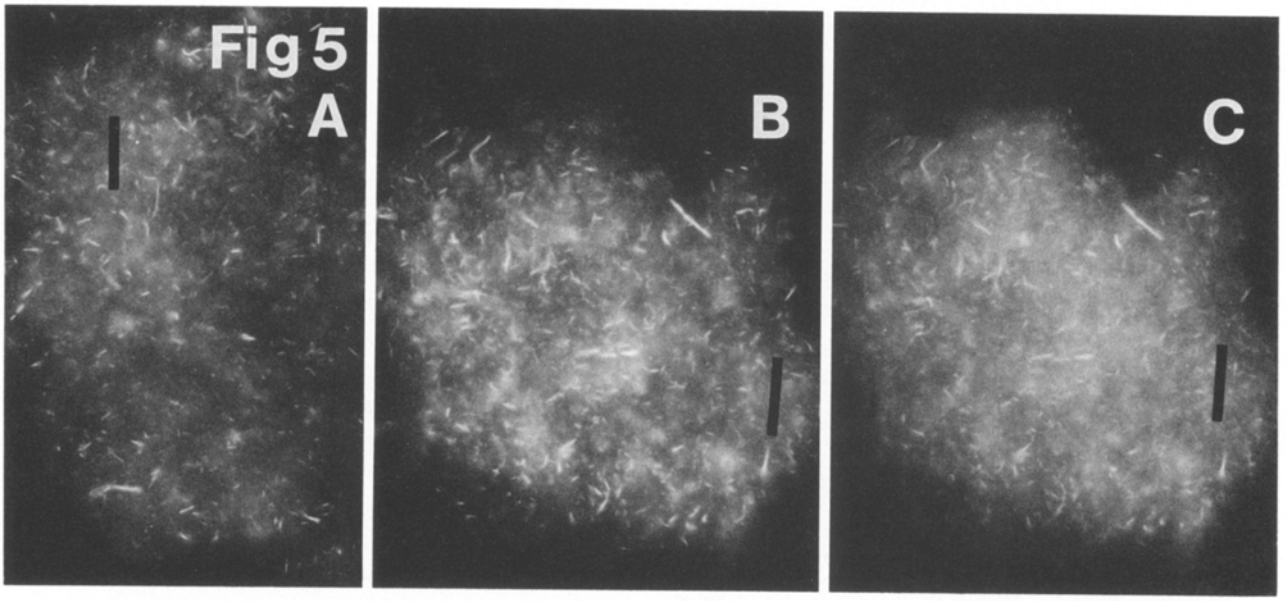

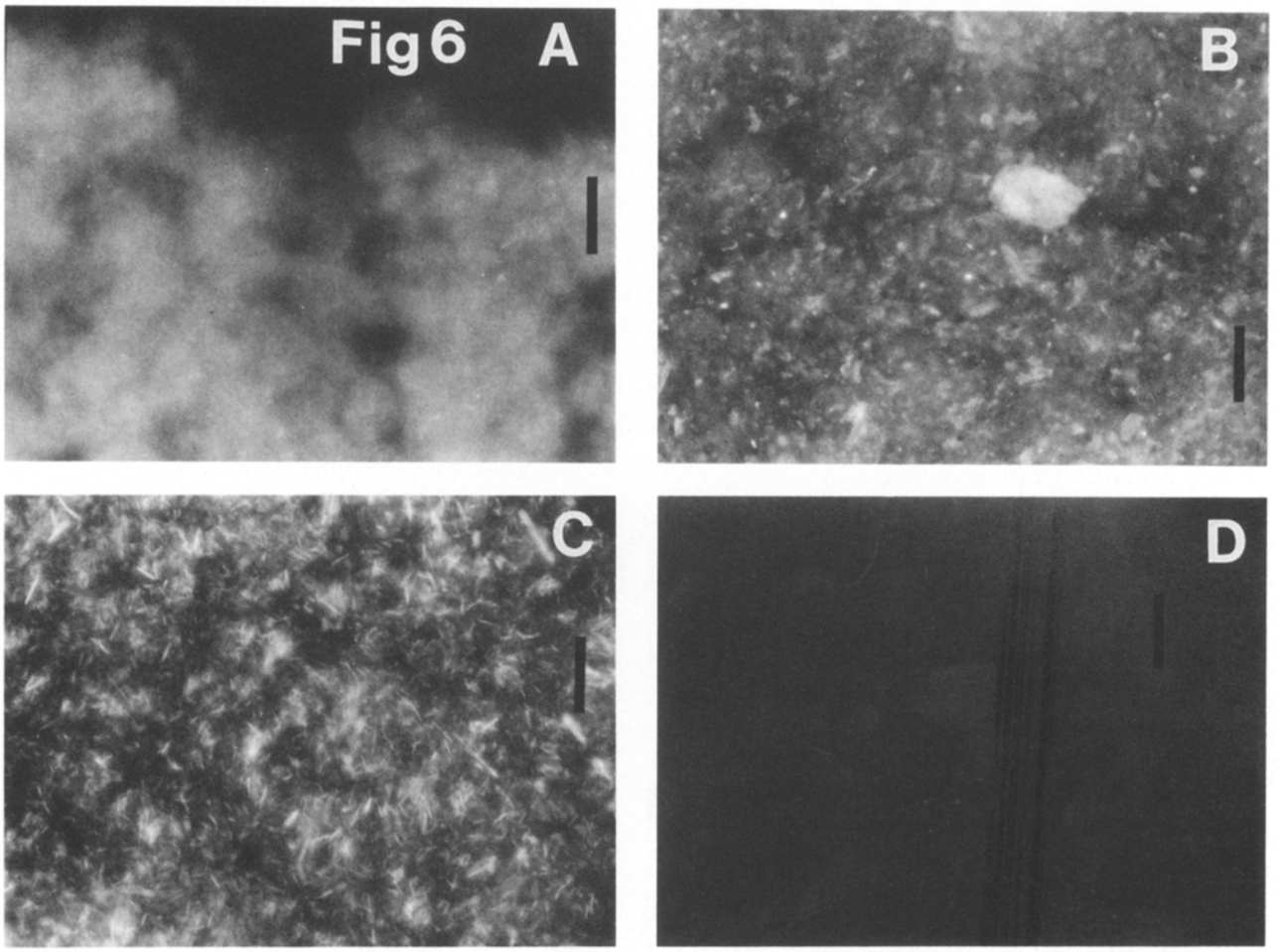

Fig. 5. Appearance of microfilaments after staining with different fluorescent stains. Tissue was ground and processed as in Fig. 2 B and the resuspended pellets were stained with: **A** fluorescein-conjugated myosin S_1; **B** and **C** double-stained with fluorescein-myosin and rhodamine-phalloidin. **A** and **C** Viewed under a blue excitation (490 nm) with a band-pass barrier filter (520–560 nm); **B** viewed under a green excitation (546 nm) with a barrier filter (580 nm). Bars: 10 μm

Fig. 6. Effect of omission from and additions to the low ionic strength extraction buffer on the yield of microfilaments. Tissue ground and processed as in Fig. 2 B, but buffer was modified as follows: **A** EGTA omitted; **B** Mg^{++} omitted: **C** PMSF omitted; **D** Mg^{++} replaced with 5 mM $CaCl_2$. Bars: 10 μm

These filaments did not seem to be an artefact of aggregation brought about by pelleting, since direct examination of the unpelleted (filtered) homogenate revealed filaments with a wide array of morphologies (Fig. 2 C–H), including straight and crenulated (Fig. 2 C) with a bright dot (arrow), bent at right angles (Fig. 2 E and F), and bent at other angles (Fig. 2 D, F, and H).

The possibility of artefacts in tissue extracts

When preparing F-actin samples for microscopy, fixatives such as paraformaldehyde are generally employed to lessen disruption or artificial aggregation. However, when preparing F-actin samples for biochemical analysis, such fixatives are unwelcome, yet attempts to isolate F-actin in their absence can lead to artefacts of Mg-induced aggregation, either via the formation of Mg-actin paracrystals (Strzelecka-Golaszewska et al. 1978) or actin polymerization (Moosecker and Tilney 1975). In addition, phalloidin, which as rhodamine-phalloidin is the preferred fluorescent stain for microfilaments, can bring about actin polymerization (Taylor and Wang 1980).

The evidence from in situ studies (Fig. 1 D and E) showing, if anything, even better preservation of microfilaments in tissues sectioned directly (without fixative) into CSB, implies, but does not prove, that artefacts are not occurring during extraction in this same buffer. In addition, the similarity between filaments in homogenates (Fig. 2 C–H) with those in situ again argues strongly against artefactual aggregation.

Nevertheless, in order to determine whether the precipitated material corresponded to Mg-actin paracrystals or to Mg-induced actin polymerization, we looked at the effects of different Mg^{++} concentrations in CSB on the yield and appearance of isolated microfilaments. With 3 mM Mg^{++}, only short, thick pieces of MF bundles were evident (Fig. 3 A), whereas with 50 mM Mg^{++}, many brightly-stained filaments were present in the pellet, but were of unusual shape (Fig. 3 B) and sometimes 2 or more appeared to be stuck together (Fig. 3 C, arrow). The sedimentability of F-actin depended on the Mg^{++} concentration of both the grinding medium and the resuspension medium. Tissue ground in 10 m Mg^{++} yielded numerous filaments when sedimented at low **g** forces (Fig. 4 A) and less at higher **g** forces (Fig. 4 B). In contrast, when the concentration of Mg^{++} in the grinding medium was 5 mM, less F-actin sedimented at low **g** forces (Fig. 4 C), and more sedimented at high **g** forces (Fig. 4 D). The easier sedimentability of F-actin in 10 mM Mg^{++} than at 5 mM seems to arise from the greater proportion of large fragments at the higher Mg^{++} level (compare Fig. 4 A with C and B with D).

These larger fragments could have resulted from artifical aggregation in 10 mM Mg^{++} or from enhanced integrity of genuine MF. These alternatives were tested by extracting tissue in CSB at 0 and 10 mM Mg^{++} and then the Mg^{++} level was maintained or adjusted to 10 or 3 mM. Adjusting 10 mM extracts to 3 mM resulted in partial fragmentation, while adjusting extracts with 0 mM added Mg^{++} to 10 mM caused no increase in size or amount of material pelleted (data not shown).

To determine whether the fluorescent material was an artefact of phalloidin-induced polymerization, we used an alternative fluorescent probe for actin, fluorescein-labelled myosin S_1 fragment. This probe, when used in the absence of phalloidin or rhodamine-phalloidin, yielded patterns of filaments (Fig. 5 A) very similar to those normally seen with rhodamine-phalloidin. Dual-labelling with rhodamine-phalloidin (Fig. 5 B) and fluorescein-myosin (Fig. 5 C) gave identical patterns, thus indicating that the labelling was specific for actin filaments.

Staining with rhodamine-phalloidin was very rapid (less than 30 s) and filament size did not change over time although the extent of staining increased slowly for about 5 min, again suggesting that phalloidin-induced polymerization was not occurring. In further support of this, pellets fixed in paraformaldehyde yielded rhodamine-phalloidin-stained fluorescent filaments indistinguishable from those obtained with unfixed samples (data not shown). In addition, pre-treatment with unlabelled phalloidin almost completely prevented binding of rhodamine-phalloidin (data not shown).

Optimal extraction conditions

Various components of the ionic strength buffer (CSB) were varied to determine which were most beneficial for the isolation of the least-fragmented filaments (bundles, cables). When EGTA was omitted from CSB, very little filamentous material was apparent, just a hazy background (Fig. 6 A). When Mg^{++} was omitted (Fig. 6 B), short, stubby fluorescent fragments were seen, and when Mg^{++} was replaced with 5 mM Ca^{++} (Fig. 6 D) no fluorescent material whatsoever was visible, while when the protease inhibitor PMSF was omitted, filaments appeared shorter (Fig. 6 C) than in regular CSB.

The presence of F-actin in low speed pellets

Additional support for the presence of actin in the putative cytoskeleton fraction comes from evidence from gel electrophoresis and Western blots. Pellets and supernatant fractions were extracted in CSB + PTE and supplemented with 2 × sample buffer, electrophoresed and either stained with Brilliant Blue or transferred to membranes. Typically stained samples and typical blots probed with actin antibody are shown in Fig. 7. Coomassie stained proteins in the 4,000 × **g** supernatant (Fig. 7, lane a) and pellet (Fig. 7, lane b; the cytoskeleton fraction) are shown, and Western blots probed with actin antibody are shown in lanes c–h. The Coommassie stained pellet (lane b) shows numerous proteins with a predominant band at 43 kDa, the expected M. Wt. of actin, while there is only a minor band at this location in the 4,000 × **g** supernatant. Standard actin is located at 43 kDa (Fig. 7, lane h) and pea actin is present in all fractions including the homogenate (Fig. 7, lane g), the 120 × **g** supernatant (Fig. 7, lane f), the 4,000 × **g** supernatant (Fig. 7, lane e), the 15,000 × **g** pellet (Fig. 7, lane d), and the 4,000 × **g** pellet (Fig. 7, lane c). Approximately 20% of the actin is pelletable, with about 80–90% of this being in the 4,000 × **g** pellet. It should be noted that the pellets are 10 × concentrated in comparison with the supernatants. There is evidence of an actin degradation product at about 33 kDa, which becomes increasingly evident when EGTA or PMSF are excluded from the extraction buffer.

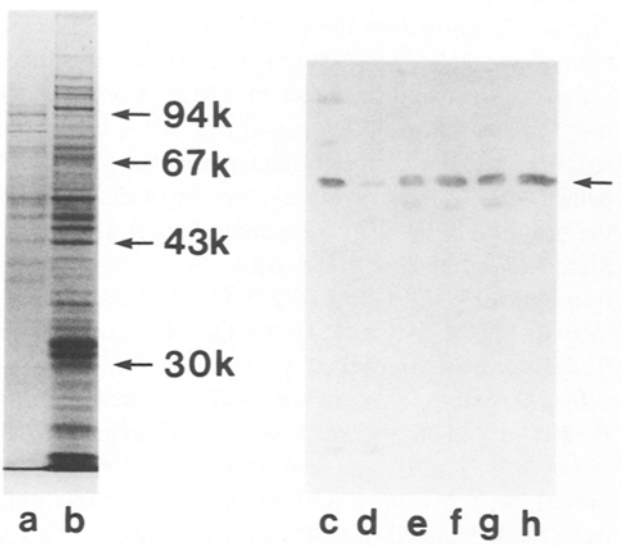

Fig. 7. Coomassie-stained gels and actin-probed Western blots of pea stem fractions. Tissue was homogenized in CSB + PTE and centrifuged sequentially at 120, 4,000, and 15,000 × **g**. Samples in CSB + PTE were mixed with 2 × sample buffer, heated for 3 min to 100 °C and electrophoresed. Coomassie-stained samples are shown for the 4,000 × **g** supernatant (**a**) and the 4,000 × **g** pellet (**b**). Western blots probed with actin antibody show samples from the 4,000 × **g** pellet (**c**), the 15,000 × **g** pellet (**d**), the 4,000 × **g** supernatant (**e**), the 120 × **g** supernatant (**f**), the homogenate (**g**), and 200 ng standard actin (**h**). Arrows show the positions of M.Wt. markers (kDa). Note: Pellets were dissolved in 0.1 vol. of CSB + PTE and so are 10 × concentrated compared with the supernatant fractions

Discussion

Both the conventional, high ionic strength buffer (MFSB) of Traas et al. (1987) and our low ionic strength buffer (CSB) showed numerous long filaments in hand-cut longitudinal sections of dark-grown pea epicotyls (Fig. 1). Such long filaments (> 100 μm) were not found in pelleted extracts, presumably because the grinding methods employed to break the cell wall also caused fragmentation (or depolymerization) of filaments. Nevertheless, we were able to show that rhodamine-phalloidin labelling of pea epicotyl tissue homogenized in CSB frequently furnished fragments of F-actin over 30 μm long (Fig. 2 B) and occasionally up to 40 μm, especially when brief, gentle homogenization was performed. However, when the high ionic strength, microfilament-stabilizing buffer of Traas et al. (1987) was used, yields of filaments were much lower and individual filaments were shorter (Fig. 2 A). Earlier work with animal tissues (Lenk et al. 1977) has shown that high concentrations of monovalent cation (100 mM NaCl) disrupt filament integrity. This could explain the low yields we achieved using MFSB (which contains 165 mM Na^+; Traas et al. 1987). In this regard, we found that the resuspension of pellets in CSB containing 100 mM or more K^+ or Na^+ caused the almost total fragmentation of microfilaments (data not shown). Furthermore, when buffers developed for the extraction of G-actin (Vahey and Scordilis 1980) were employed for homogenization of pea tissue, no such filaments were visible (data not shown).

The thickness of the isolated filaments seems consistent with that seen in situ. Some were as thick as 600–700 μm (Fig. 2 B) and might have arisen from fragmentation of peripheral filament cables (Fig. 1 B), others appeared to be about 200 μm thick and might have arisen from filament bundles traversing the cytoplasm (Fig. 1 E). However, it is often difficult to estimate exact thickness because the fluorescent image is not the same as the actual filament, and difficult to track their entire length because they do not stay in the same focal plane (Parthasarty 1985). It should be noted that the filaments in the pellet did not appear to be packed together and

might have been separated by some intervening materials, thus rendering it unlikely that they had sedimented as aggregates. The morphology of filaments from unpelleted homogenates (Fig. 2 C–H) was amazingly similar to filaments viewed in situ (Fig. 1), with some being straight (Fig. 2 C), others curved (Fig. 2 D and G), others with right-angle bends (Fig. 2 E and H), and still others with more obtuse angles (Fig. 2 F and H).

For the purpose of this paper, which was to develop methods for the isolation, in high yield, of relatively intact microfilaments, a compromise had to be made between filament integrity and yield. When we gently crushed tissue directly on a microscope slide and immediately stained it, we could invariably find large, semi-intact cytoskeletons released from the broken cells, but yields of such cytoskeletons were exceedingly low (data not shown). Long-term (>30 s) grinding in a mortar and pestle produced the largest total yield, but the filaments were badly fragmented. Accordingly, a brief (5–10 s) homogenization was employed here as a compromise to give reasonably high yields of semi-intact filaments.

These isolated filaments do not appear to be artefacts arising from either Mg^{++}-induced polymerization or aggregation of F-actin, both of which are situations we were attempting to avoid on the assumption that the less the artefacts engendered during microfilament isolation, the more likely the actin-associated components would be genuine. Once again, a compromise had to be made, this time between conditions leading to aggregation and conditions leading to depolymerization of F-actin. We found that levels of Mg^{++} below 3 mM (Figs. 3 and 6 C) led to a drastic reduction in size and yield of pelletable filaments, levels greater than 25 mM led to increased thickness of filaments (Fig. 3), while 5 to 10 mM gave the greatest yield of the most intact filaments. These results with pea epicotyls tissue are in amazingly close agreement with the report of Mooseker and Tilney (1975) working with chicken intestinal cells. These workers attributed the reduction in yield at low (<3 mM) levels of Mg^{++} to actin depolymerization (destabilization), and the increased stability at high levels (15–40 mM) to Mg-actin polymerization. These workers, using evidence from electron microscopy, also found that 5 to 10 mM Mg^{++} was the best compromise between depolymerization and polymerization (Mooseker and Tilney 1975). It has been shown that F-actin from plants needs levels of Mg^{++} of 5 mM or higher to maintain filament integrity/stability in situ (Vaughan and Vaughan 1987). Furthermore, Metcalf et al. (1984) used buffers containing 50 mM Mg^{++} in the analysis of fluid squeezed out of soybean tissue yet presented pictures of normal-looking filaments as judged by electron microscopy. The increased thickness of filaments isolated in high Mg^{++} buffers (Fig. 3 C) may have been the result of side-by-side aggregation elicited by an array of divalent cations at elevated concentrations (Strzelecka-Golaszewska et al. 1978). Additional evidence that these filaments were not aggregates of Mg-actin precipitation comes from the studies with homogenates examined directly, i.e., without pelleting. In these experiments, individual filaments were clearly dispersed (Fig. 2 C–H).

These isolated, easily-pelletable filaments do not appear to be an artefact arising from phalloidin-induced polymerization (Taylor and Wang 1980), since very similar pictures were obtained when pellets were stained with fluorescein-conjugated S_1-myosin in the absence of any phalloidin derivative (Fig. 3 A). All the evidence points to them being genuine F-actin filaments, since co-staining with fluorescein-S_1 myosin and rhodamine-phalloidin revealed identical patterns (compare Fig. 3 B with C) and pre-staining with unlabelled phalloidin almost totally prevented subsequent staining with rhodamine-phalloidin.

Our results show that the plant cytoskeleton, like the animal cytoskeleton, is very sensitive to proteolytic degradation, since the omission of PMSF from the extraction medium resulted in a drastic reduction in the size and number of microfilaments in the low speed pellet (Fig. 6 C). Furthermore, omission of EGTA from the grinding buffer led to the almost total absence of filaments in the low speed pellet, with only a hazy fluorescence being visible (Fig. 6 A), while the replacement of Mg^{++} by Ca^{++} (Fig. 6 D) led to virtually no fluorescence in the pellet. In this context, we have shown that about 20% of the total actin sediments as F-actin at 4,000 × **g**, relatively little sediments at 15,000 × **g** (Fig. 7), and almost none at 100,000 × **g** (not shown). We have noticed that various fractions from tissue isolated in CSB in the presence of EGTA yield a dominant band at 43 kDa and a minor band at 33 kDa both of which react with actin antibody on Western blots (Fig. 7). However, extraction in the absence of EGTA yields essentially no undegraded actin and just the degradation product at 33 kDa (data not shown), exactly the size reported for proteolysis of actin in skeletal muscle (Mornet and Ue 1984). Perhaps there is a Ca-activated protease in peas which degrades actin akin to the Ca-activated protease in ascites tumor cells which degrades vimentin (Nelson and Traub 1982).

Acknowledgements

This research was supported by NSF #DCB-8802167 and #DCB-9007729, the University of Nebraska Research Council, and the University of Nebraska Center for Biotechnology (to ED); the Japanese Ministry of Education, Science and Culture, and Calsonic Inc. of Tokyo, Japan (to SA). We thank Dr. M. V. Parthasarathy, Cornell University, for his critical comments on an earlier version of this manuscript, and Ms. Yuko Ito, Ehime University, for the Western blots.

References

Bershadsky AG, Vasilev JM (1988) Cytoskeleton. Plenum, New York [Siekevitz P (ed) Cellular organelles]

Capco DG, Munoz DM, Gassmann CJ (1987) A method for analysis of the detergent-resistant cytoskeleton of cells within organs. Tissue Cell 19: 607–616

Davies E, Schuster AM (1981) Intercellular communication in plants: evidence for a rapidly-generated, bidirectionally-transmitted wound signal. Proc Natl Acad Sci USA 78: 2422–2426

Giloh H, Sedat JW (1982) Fluorescence microscopy: reduced photobleaching of rhodamine and fluorescein protein conjugates by n-propyl gallate. Science 217: 1252–1255

Lenk R, Ransom L, Kaufmann Y, Sheldon S (1977) A cytoskeletal structure with associated polyribosomes obtained from HeLa cells. Cell 10: 67–78

Ma Y-Z, Yen L-F (1989) Actin and myosin in pea tendrils. Plant Physiol 89: 586–589

Metcalf TN III, Sabo LJ, Schubert KR, Wang JL (1984) Ultrastructural and immunochemical analyses of the distribution of microfilaments in seedlings and plants of *Glycine max*. Protoplasma 120: 91–99

Mooseker MS, Tilney LG (1975) Organization of an actin filament-membrane complex. J Cell Biol 67: 725–743

Mornet D, Ue K (1984) Proteolysis and structure of skeletal muscle actin. Proc Natl Acad Sci USA 81: 3680–3684

Nelson WJ, Traub P (1982) Effect of the ionic environment on the incorporation of the intermediate-sized filament protein vimentin into residual cell structures upon treatment of Ehrlich ascites tumour cells with Triton X-100 II. Ultrastructural analysis. J Cell Sci 53: 77–95

Nothnagel EA, Barak LS, Sanger JW, Webb WW (1981) Fluorescence studies on modes of cytochalasin B and phallotoxin action on cytoplasmic streaming in *Chara*. J Cell Biol 88: 364–372

Parthasarathy MV (1985) F-actin architecture in coleoptile epidermal cells. Eur J Cell Biol 39: 1–12

Picciolo GL, Kaplan DS (1984) Reduction of fading of fluorescent reaction product for microphotometric quantitation. Adv Appl Microbiol 30: 197–234

Schmit A-C, Lambert A-M (1987) Characterization and dynamics of cytoplasmic F-actin in higher plant endosperm cells during interphase, mitosis, and cytokinesis. J Cell Biol 105: 2157–2166

Schuster A, Davies E (1983) Protein and RNA metabolism in pea epicotyls. I. Changes during aging. Plant Physiol 73: 809–816

Seagull RW (1989) The plant cytoskeleton. CRC Crit Rev Plant Sci 8: 131–167

Staiger CJ, Schliwa M (1987) Actin localization and function in higher plants. Protoplasma 141: 1–12

Strzelecka-Golaszeska H, Prochniewicz E, Drabikowski W (1978) Interaction of actin with divalent cations. 1. The effect of various cations on the physical state of actin. Eur J Biochem 88: 219–227

Taylor DL, Wang Y-L (1980) Fluorescently labelled molecules as probes of the structure and function of living cells. Nature 284: 405–410

Tewinkel M, Kruse S, Quader H, Volkman D, Sievers A (1989) Visualization of actin filament pattern in plant cells without prefixation. A comparison of differently modified phallotoxins. Protoplasma 149: 178–182

Traas JA, Doonan JH, Rawlins DJ, Shaw PJ, Watts J, Lloyd CW (1987) An actin network is present in the cytoplasm throughout the cell cycle of carrot cells and associates with the dividing nucleus. J Cell Biol 105: 387–395

Vahey M, Scordilis SP (1980) Contractile proteins from tomato. Can J Bot 58: 797–801

Vaughan MA, Vaughan KC (1987) Effects of microfilament disrupters on microfilament distribution and morphology in maize root cells. Histochemistry 87: 129–137